

Localization of spinons in random Majumdar-Ghosh chains

Arthur Lavarélo and Guillaume Roux

LPTMS, Univ. Paris-Sud, CNRS, UMR8626, F-91405 Orsay, France.

(Dated: May 31, 2018)

We study the effect of disorder on frustrated dimerized spin-1/2 chains at the Majumdar-Ghosh point. Using variational methods and density-matrix renormalization group approaches, we identify two localization mechanisms for spinons which are the deconfined fractional elementary excitations of these chains. The first one belongs to the Anderson localization class and dominates at the random Majumdar-Ghosh (RMG) point. There, spinons are almost independent, remain gapped, and localize in Lifshitz states whose localization length is analytically obtained. The RMG point then displays a quantum phase transition to phase of localized spinons at large disorder. The other mechanism is a random confinement mechanism which induces an effective interaction between spinons and brings the chain into a gapless and partially polarized phase for arbitrarily small disorder.

PACS numbers: 75.10.Kt, 75.40.Mg, 75.10.Jm, 75.10.Pq

Spinons are fractional excitations corresponding to half of a spin excitation in quantum magnets. They typically appear in understanding the excitation spectrum of one-dimensional systems such as the frustrated $J_1 - J_2$ Heisenberg chain. This model possesses an exact ground-state at the Majumdar-Ghosh (MG) point $J_1 = 2J_2$ [1] which is the prototype of a valence bond solid (VBS) state and for which a variational approach describes well elementary excitations [2]. Further, spinons play a crucial role in unconventional two-dimensional phase transitions in which they could be deconfined [3]. Investigating the effect of disorder on their dynamics is all the more essential, since randomness is inherent to experimental samples. Possible strategies to study random quantum magnets are bosonization [4], provided the disorder is small, or real-space renormalization group (RSRG) [5], rather suited for the strong disorder regime. The latter is asymptotically exact in the case of an infinite-disorder fixed point [6], but when it converges to a finite-disorder fixed point, its outcome can be questioned at small disorder. Numerical approaches are challenging due to strong finite-size effects from rare events [7] and the interplay between frustration and disorder cannot be addressed using the powerful quantum Monte-Carlo method because of the sign problem. Lastly, most studies on random magnets focus on the ground-state while little is known about the fate of elementary excitations. So far, it has been conjectured [8] that the gap of frustrated dimerized chains is broken by a domain formation mechanism similar to the one suggested for Mott phases [9]. Later, RSRG studies [10] found that it would belong to the class of the large-spin phase [11].

In this Letter, two localization mechanisms at play in random frustrated dimerized chains are unveiled using a variational approach supported by density-matrix renormalization group (DMRG) calculations [12]. They provide both quantitative predictions and an intuitive picture of the physics. The first mechanism belongs to the Anderson class and governs the dynamics of a spinon at the random Majumdar-Ghosh (RMG) point which generalizes the MG condition in the presence of random bonds. Increasing disorder at the RMG point induces a transition to a paramagnetic phase of localized spinons. The second one is a random confinement which generates an effective interaction between spinons which stabilizes the formation of domains and breaks the spin gap.

Model – We consider a frustrated dimerized spin-1/2 chain with random nearest-neighbor couplings α_i and next-nearest neighbor couplings β_i :

$$\mathcal{H} = \sum_i \alpha_i \mathbf{S}_i \cdot \mathbf{S}_{i+1} + \beta_i \mathbf{S}_{i-1} \cdot \mathbf{S}_{i+1}, \quad (1)$$

where \mathbf{S}_i are spin-1/2 operators. In the following, the average couplings are written $\overline{\alpha}_i = \alpha$ and $\overline{\beta}_i = \beta$ with $\alpha = 2\beta$ to start from the usual MG point. When applying \mathcal{H} on MG states $|\text{MG}\rangle = |\cdots \bullet\bullet \bullet\bullet \bullet\bullet \bullet\bullet \bullet\bullet \cdots\rangle$ with dimers $|\bullet\bullet\rangle = \frac{1}{\sqrt{2}}[|\uparrow\downarrow\rangle - |\downarrow\uparrow\rangle]$, it can be shown [8, 13] that the latter remain degenerate eigenstates of the Hamiltonian provided

$$\alpha_i = \beta_i + \beta_{i+1}, \quad (2)$$

which we call the random Majumdar-Ghosh (RMG) point. It imposes a local correlation between the random couplings. The two localization mechanisms stem from the splitting of the Hamiltonian into $\mathcal{H} = \mathcal{H}_{\text{RMG}} + \mathcal{H}_{\text{dim}}$, where \mathcal{H}_{RMG} follows (2) and \mathcal{H}_{dim} is the remaining part (see below).

Localization at the RMG point – An effective model for the dynamics of a spinon is obtained assuming (2) by considering an open chain with an odd number of sites and spinon states $|j\rangle = |\cdots \bullet\bullet \uparrow \bullet\bullet \cdots\rangle$ with a free spin at site $2j+1$ separating two MG domains. By projecting [13] \mathcal{H}_{RMG} orthogonally onto the free family of non-orthogonal states $\{|j\rangle\}$, the effective spinon Hamiltonian reads

$$\left(\tilde{\mathcal{H}}_{\text{RMG}} - E_{\text{MG}}\right) |j\rangle = \frac{\beta_{2j+1}}{2} \left(|j-1\rangle + \frac{5}{2}|j\rangle + |j+1\rangle\right), \quad (3)$$

where $E_{\text{MG}} = -\frac{3}{4} \sum_i \beta_i$ is the MG state energy extrapolated to odd sizes. Consequently, the motion of the spinon, taking place either on odd or even site sublattices, obeys a special kind of Anderson Hamiltonian expected to induce localization. The matrix of $\tilde{\mathcal{H}}_{\text{RMG}}$ is non-hermitian because $\{|j\rangle\}$ is not orthogonal but is similar to a hermitian matrix [13]. Yet, tridiagonal form is well suited to the Dyson-Schmidt method [14, 15]. By writing $|\psi\rangle = \sum_j \psi_j |j\rangle$ the spinon variational wave-function and $\tilde{\beta}_j \equiv \beta_{2j+1}$, we introduce the Riccati variables $R_j = \psi_{j+1}/\psi_j$ to rewrite Schrödinger's equation as

$$R_j + 5/2 + 1/R_{j-1} = 2E/\tilde{\beta}_j, \quad (4)$$

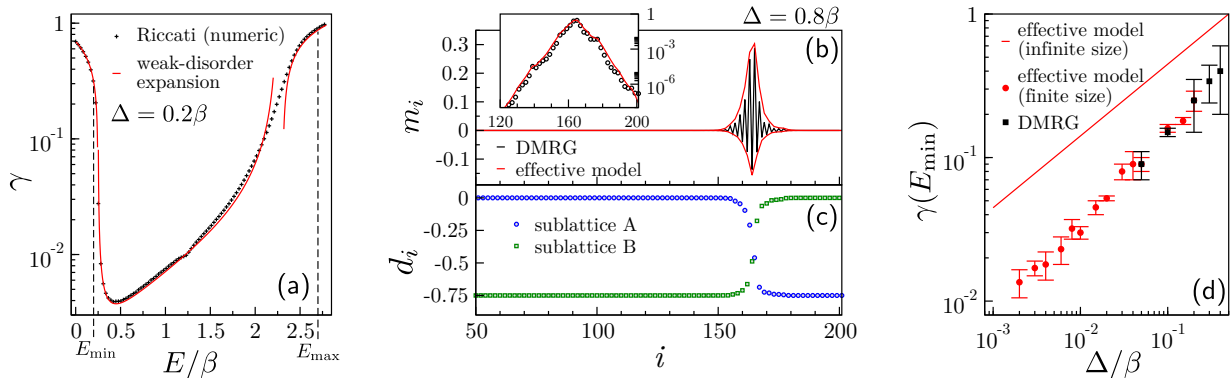


FIG. 1. (color online) *At the RMG point* : (a) Lyapunov exponent γ vs energy E of the effective model. (b) magnetization profile from DMRG in sector $S^z = 1/2$. Inset: log plot. (c) dimerization profile showing the MG domains. (d) finite size effects on the Lyapunov exponent.

for a given spinon energy E . The integrated density of states $N(E)$ and Lyapunov exponent $\gamma(E)$ of a single spinon excitation are obtained by extending the energy to the complex plane. Assuming that the probability density of the Riccati variables converges toward an invariant distribution of measure $dW(R)$ as $j \rightarrow \infty$, the characteristic function

$$\Omega(z) = \int dW(R) \ln R \quad (5)$$

is such that $\Omega(E + i0^+) = \gamma(E) + i\pi(1 - N(E))$. These quantities can be obtained either numerically or analytically from a weak-disorder expansion [16] as described below. In the non-disordered case, the spinon dispersion relation is $E(k) = \beta(5/4 + \cos k)$ with k the momentum. By introducing the variables

$$y_j = \left[1 + \frac{y_{j-1} - 1}{1 + g_j(y_{j-1} - 1)} \right] e^{-2ik}, \quad g_j = \frac{E(k)}{i \sin k} \left(\frac{1}{\beta} - \frac{1}{\tilde{\beta}_j} \right),$$

it can be shown that the first term in the expansion in the first moment of the g -distribution gives $\Omega \simeq ik - \overline{g^2}/2$. Specializing to the case of a uniform distribution over $[\beta - \Delta, \beta + \Delta]$, the explicit calculation for energies $E < \beta/4$ gives [13]

$$\gamma(E) = \text{arccosh} \left[\frac{5}{4} - \frac{E}{\beta} \right] - \frac{1}{6} \frac{E^2}{(E - \frac{5}{4}\beta)^2 - \beta^2} \left(\frac{\Delta}{\beta} \right)^2. \quad (6)$$

The result is compared to numerics on Fig 1(a). In particular, we obtain that the RMG spinon localization length $\xi_{\text{RMG}} = 1/\gamma(E_{\min})$ in the state with the lowest energy $E_{\min} = \beta_{\min}/4$ (where $\beta_{\min} = \min \tilde{\beta}_j$), scales as:

$$\xi_{\text{RMG}} \simeq \sqrt{2\beta/\Delta}. \quad (7)$$

Notice that ξ_{RMG} cannot be captured by RSRG and is not related to the spin correlation length of a MG state.

Another important outcome of the effective model is that it provides hints on the finite-size effects on the spinon energies, with consequences on the spin gap and the localization length. The lowest energy spinon states correspond to the regime of Lifshitz localization, in the tail of the density of states and

controlled by a rare-events scenario. Adapting Lifshitz argument [15, 17], a region of length ℓ with many $\tilde{\beta}_j$ close to β_{\min} – i.e. provided $|\tilde{\beta}_j - \beta_{\min}| \leq C(E_\ell - E_{\min})$ for all j in the region, with C a constant – has its lowest energy of the order of $E_\ell \simeq E_{\min} + \beta_{\min} \pi^2 / 2\ell^2$, assuming $\beta_{\min} > 0$ and writing $E_{\min} = \beta_{\min}/4$. Since the probability of creating such region scales as $P_\ell \propto [C(E_\ell - E_{\min})/2\Delta]^\ell$ for a uniform distribution, the low-energy behavior of the integrated density of states is

$$N(E) \propto \exp \left\{ -\pi \sqrt{\frac{\beta_{\min}/2}{E - E_{\min}}} \ln \left(\frac{2\Delta/C}{E - E_{\min}} \right) \right\}. \quad (8)$$

This behavior is in very good agreement with the numerics on the effective model [13]. Regarding finite-size effects on the spinon energy E_L in a chain of length L , the probability to have the minimum energy must be such that $P_\ell \sim 1/L$. This yields $N(E_L) \sim 1/L$ in Eq. (8), again in good agreement with numerical results [13]. Asymptotically, we thus expect finite-size corrections of the form $E_L \simeq E_{\min} + K\beta_{\min}(\ln(\ln L)/\ln L)^2$ with K a constant.

In order to validate this effective model, we compare it to accurate DMRG calculations of the magnetization profile in a chain with total spin $S^z = 1/2$ with the effective model predictions where $m_i \equiv \langle S_i^z \rangle$ is deduced from the ψ_j [13]. As judged by the results of Fig. 1(b), the effective model provides quantitative predictions of the magnetization profile. From the local dimerization pattern $d_i = \langle \mathbf{S}_i \cdot \mathbf{S}_{i+1} \rangle$ of Fig. 1(c), the localized spinon clearly separates two different MG domains. One can extract the actual ξ_{RMG} from DMRG profiles. On Fig. 1(d), strong deviations between DMRG calculations and the infinite size result (7) are observed. This difference actually originates from finite-size effects : one has to take $\xi_{\text{RMG}} = 1/\gamma(E_L)$ on a finite system, which yields strong deviations, even for large sizes.

Spin gap and transition to a paramagnetic state – From these results on single spinon excitations, we can infer the behavior of the spin gap at the RMG point with increasing disorder. The MG states remain degenerate ground-states at small enough disorder and the lowest triplet excitation above them is to create two localized spinons in each sublattice (see Fig. 2(a-b)) with both the minimal energy E_{\min} . As the

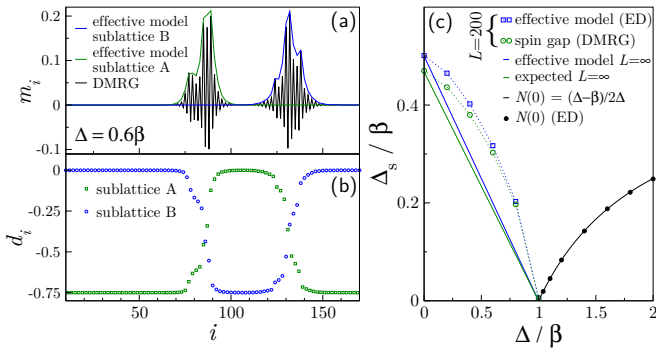


FIG. 2. (Color online) *At the RMG point* – typical magnetization (a) and dimerization (b) profiles in the lowest triplet excited state for $\Delta < \beta$. (c) evolution of the minimum spin gap (see text for details), and spinon density $N(0)$, v.s. the disorder strength Δ .

two spinons are localized on very large clusters, the singlet and triplet gaps must be degenerate in the thermodynamical limit [18]. Consequently, the effective model prediction for the spin gap is $\Delta_S^{\text{eff}} = \beta_{\text{min}}/2 = (\beta - \Delta)/2$. In order to give a typical finite-size behavior, we show on Fig. 2(c) the minimum DMRG triplet gap found over an hundred of samples of chains of size $L = 200$, compared with the effective model result on the same samples. Two main features come out. First, the difference between the two finite-size curves can be attributed to the variational error, already making the non-disordered spin gap Δ_S^0 smaller than Δ_S^{eff} . As Lifshitz states correspond to large ‘clean’ boxes with couplings β_{min} , the same correction should apply to them, improving the prediction to $\Delta_S = \Delta_S^0(1 - \Delta/\beta)$ (label ‘expected $L = \infty$ ’ on Fig. 2(c)). Second, the curved nature of the typical spin gap for $L = 200$ and randomly chosen samples is due to the fact that the minimum gap discussed above is obtained for extremely rare events and can be viewed as a sort of finite-size effect since Δ_S is not self-averaging.

Increasing further the disorder strength, the spin gap vanishes for $\beta = \Delta$ for which E_{min} becomes negative ($E_{\text{min}} = 9\beta_{\text{min}}/4$ for $\beta_{\text{min}} < 0$) so that states with two or more spinons get energetically favored. The MG states are still eigenstates but no longer ground-states. The resulting picture shortly after the critical point is a paramagnetic phase of localized spinons, as we can neglect tiny residual magnetic couplings between spinons for a small enough density. This spinon density is nothing but the density of negative energy spinon states $N(0)$. Therefore, the magnetic susceptibility must change from zero to $\chi \sim N(0)$ across the transition as depicted in Fig. 2(c). DMRG calculations do confirm this picture, showing that the ground and first excited states are nearly degenerate states with localized spinons. Within the effective model picture, the quantum phase transition from the gapped to the paramagnetic phase is located at $\beta_{\text{min}} = 0$ and its order depends on the disorder distribution. A continuous transition occurs for a continuous disorder distribution while binary disorder yields a first order transition. In order to determine $N(0)$ for the effective model, one must realize that the Lifshitz argument cannot be used for spinon energies close to zero [13].

Yet, we argue that the number of negative energy states is actually given by the number of negative $\tilde{\beta}_j$ which, for the box distribution, gives $N(0) = (\Delta - \beta)/(2\Delta)$. The associated critical exponent of the susceptibility is thus one. This argument is checked numerically on the effective model in Fig. 2(c). Checking this law using DMRG is particularly difficult as the spinon density gets very small close to the critical point. Lastly, we point out that this low spinon density picture fails at larger disorder (large spinon density) for two related reasons: magnetic couplings between spinons become non-negligible and the neglecting states with non-local dimers is questionable. It is likely that the spinon phase then becomes partially polarized and connected to the large-spin phase that exists away from the RMG point and that we now discuss.

Random confinement localization – Moving away from the RMG point (2) is progressively done by uncorrelating the α_i and β_i through the introduction of random variables δ_i , uncorrelated to the β_i , and such that

$$\alpha_i = (1 - \lambda)(\beta_i + \beta_{i+1}) + \lambda\delta_i, \quad (9)$$

where $\overline{\delta_i} = 2\beta$ and $\lambda \in [0, 1]$ is a tuning parameter. The correlations $\overline{\alpha_i\beta_i} - \overline{\alpha_i}\overline{\beta_i} = (1 - \lambda)\sigma_\beta^2$ (σ^2 denoting a variance) show that the α s and β s get uncorrelated for $\lambda = 1$. As $\sigma_\alpha^2 = 2(1 - \lambda)^2\sigma_\beta^2 + \lambda^2\sigma_\delta^2$, we further impose $\sigma_\alpha^2 = 2\sigma_\beta^2$ to study the effect of the correlations only by keeping the disorder strength as for the RMG point. Lastly, using this decoupling, the Hamiltonian splits into two parts $\mathcal{H} = \mathcal{H}_{\text{RMG}} + \lambda\mathcal{H}_{\text{dim}}$, where \mathcal{H}_{dim} is a random dimerization term:

$$\mathcal{H}_{\text{dim}} = \sum_i \eta_i \mathbf{S}_i \cdot \mathbf{S}_{i+1}, \quad (10)$$

with $\eta_i = \delta_i - \beta_i - \beta_{i+1}$ random couplings of mean-value $\overline{\eta_i} = 0$. The effect of \mathcal{H}_{dim} is to localize spinons via a random confinement mechanism that can be understood within the effective model approach. The associated effective Hamiltonian $\tilde{\mathcal{H}}_{\text{dim}}$ in the single spinon basis takes a rather complicated form [13], with a dense-matrix representation. Still, its main effect is to induce an effective random chemical potential μ_i for the spinon which reads

$$\mu_i = \langle i | \mathcal{H}_{\text{dim}} | i \rangle = -\frac{3}{4} \left(\sum_{n=0}^{i-1} \eta_{2n+1} + \sum_{n=i+1}^{(L-1)/2} \eta_{2n} \right). \quad (11)$$

It is the sum of two independent random walks (the η s on each sublattice) constrained to have a total fixed length. Such a potential typically has a minimum in the bulk of large chains and create a well which localizes the spinon. As for explicitly dimerized chains [19, 20], moving away from the minimum of the potential is locally analogous to a linear confinement. DMRG calculations are nicely fitted by diagonalizing the full effective hamiltonian $\tilde{\mathcal{H}}$ matrix [13]. The location of the spinon is found to be governed by the μ_i . If one now takes the full Hamiltonian, finite-size systems display a crossover between Anderson localization at very small λ and random confinement localization which dominates up to $\lambda = 1$. It is also clear that the random confinement can stabilize many spinons states leading to the formation of many domains.

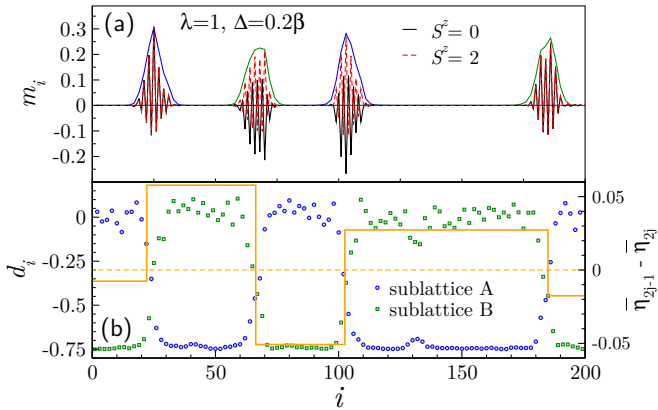


FIG. 3. (Color online) (a) Magnetization profile of a MG chain with uncorrelated couplings displaying localized spinons. Lines are the effective model predictions on each sublattices. (b) Dimerization pattern and corresponding average of the random η -dimerization term of Eq. (12) over MG domains (orange line).

MG domain formation – At small λ , \mathcal{H}_{dim} acts as a perturbation which locally lifts the degeneracy between the two MG states, as suggested qualitatively in Ref. 8. Clearly, MG states are no longer eigenstates since high order terms in perturbation theory put weights on long dimer states $|[2i-1, 2j]\rangle = | \cdots \overset{\curvearrowright}{\cdots} \cdots \rangle$ with a dimer on bond $(2i-1, 2j)$. More than dressing the MG state, the random dimerization actually destroys the spin gap as soon as $\lambda \neq 0$ and $\sigma_\beta \neq 0$. Indeed, the energy difference $\delta E_{ij} = \langle [2i-1, 2j] | \mathcal{H} | [2i-1, 2j] \rangle - E_{\text{MG}}$ between $|[2i-1, 2j]\rangle$ and the corresponding MG state reads [13]

$$\delta E_{ij} = \frac{3}{4}(\beta_{2i-1} + \beta_{2j}) - \lambda \frac{3}{4} \sum_{n=2i-1}^{2j-1} (-1)^n \eta_n. \quad (12)$$

The first term which averages to $\frac{3}{2}\beta$ stems from the cost of creating two domain walls (spinons). The second term corresponds to an effective long range interaction between the two spinons and arises from \mathcal{H}_{dim} . It averages to zero but rare events can definitely bring this state to a lower energy than the MG state: in an infinitely large system, it is always possible to find a region with η_n that do not compensate and such that the random interaction scales as the region size to make $\delta E_{ij} < 0$. At low disorder, regions must be large and the spinons far away so that their remaining magnetic coupling vanishes. The spin gap is then immediately broken.

In order to support this picture, we perform DMRG calculations for $\lambda \neq 0$ and do observe that, on a finite-system, the spin gap is strongly reduced by increasing λ , or by increasing Δ at fixed λ . We exhibit in Fig. 3(a) a sample with

$\lambda = 1$ where four spinons are present in the ground-state and for which the spin gap is zero within numerical accuracy. To complete the description, the magnetization profile along each domain wall is pretty well reproduced by using the local effective Hamiltonian for a single spinon (Born-like approximation). Finally, the averaged of \mathcal{H}_{dim} in each domain, plotted in Fig. 3(b), supports the pinning mechanism of the MG domains. The scaling of the spinon density with disorder is a challenging issue as it requires the minimization of the energy of several correlated domains which number is not fixed [21].

At low spinon densities, the ground-state is a network of localized spinons which interact via their spin degrees of freedom. The effective magnetic couplings should range from almost zero to finite values if two spinons happen to be close. There is no constraint on their signs: both ferromagnetic and anti-ferromagnetic couplings exist, making the phase partially polarized. Interestingly this weak disorder picture is physically connected with the strong disorder picture of RSRG.

Comparison with RSRG – It is interesting to compare these results with the RSRG method best suited to the strong disorder limit. From the RSRG equations given in the supplementary material, we notice that the degeneracy of the MG domains at the RMG point translates into an instability of the RSRG decimation. As soon as $\lambda \neq 0$, the gap distribution in the system converges toward an invariant power-law distribution with a non-universal exponent, characteristic of Griffith phase similar to previous results [10]. Indeed, due to frustration, the RSRG equations generate a few effective ferromagnetic couplings [13], building up a large-spin phase [11]. This supports a continuous phase from weak to strong disorder. Moreover, we stress that the non-crossing dimer basis is deeply related to the RSRG picture that targets the most probable dimer configuration from the coupling distribution.

Conclusion – This work provides quantitative results on the interplay between frustration and disorder in random MG chains. We identify two mechanisms at play for single spinon: an unusual Anderson localization mechanism, and a random confinement mechanism. The immediate destruction of the spin gap upon putting disorder is to be contrasted with its robustness for the explicitly dimerized or spin-1 chains which have a non-degenerate ground-state [22]. The presence of degenerate MG states makes the system very sensitive to disorder. We expect the same phenomenology to play a role in other random VBS, which could be witnessed using numerical methods working in the spinon basis [23]. Lastly, these mechanisms demonstrate how random couplings generate “free spins” in VBS, without vacancies or adatoms, and are thus experimentally relevant.

We thank N. Laflorencie, J.-M. Luck, C. Monthus, C. Sire and C. Texier for insightful discussions. We acknowledge support from grant ANR-2011-BS04-012-01 QuDec.

[1] C. Majumdar and D. Ghosh, J. Math. Phys. **10**, 1388 (1969); J. Math. Phys. **10**, 1399 (1969).

[2] B. S. Shastry and B. Sutherland, Phys. Rev. Lett. **47**, 964

(1981); W. J. Caspers, K. M. Emmett, and W. Magnus, J. Phys. A: Math. Gen. **17**, 2687 (1984).

[3] T. Senthil, A. Vishwanath, L. Balents, S. Sachdev, and M. P. A.

- Fisher, *Science* **303**, 1490 (2004); A. W. Sandvik, *Phys. Rev. Lett.* **98**, 227202 (2007).
- [4] T. Giamarchi, *Quantum Physics in one Dimension* International series of monographs on physics Vol. 121 (Oxford University Press, Oxford, UK, 2004).
- [5] S.-k. Ma, C. Dasgupta, and C.-k. Hu, *Phys. Rev. Lett.* **43**, 1434 (1979); C. Dasgupta and S.-k. Ma, *Phys. Rev. B* **22**, 1305 (1980); F. Iglói and C. Monthus, *Physics Reports* **412**, 277 (2005).
- [6] D. S. Fisher, *Phys. Rev. B* **50**, 3799 (1994); *Phys. Rev. B* **51**, 6411 (1995).
- [7] F. Iglói, R. Juhász, and H. Rieger, *Phys. Rev. B* **61**, 11552 (2000); N. Laflorencie, H. Rieger, A. W. Sandvik, and P. Henelius, *Phys. Rev. B* **70**, 054430 (2004).
- [8] Kun Yang, R. A. Hyman, R. N. Bhatt, and S. M. Girvin, *J. Appl. Phys.* **79**, 5096 (1996).
- [9] R. Shankar, *Int. J. Mod. Phys. B*, **04**, 2371 (1990); H. Pang, S. Liang, and J. F. Annett, *Phys. Rev. Lett.* **71**, 4377 (1993).
- [10] J. A. Hoyos and E. Miranda, *Phys. Rev. B* **69**, 214411 (2004); C. A. Lamas, D. C. Cabra, M. D. Grynberg, and G. L. Rossini, *Phys. Rev. B* **74**, 224435 (2006).
- [11] E. Westerberg, A. Furusaki, M. Sigrist, and P. A. Lee, *Phys. Rev. B* **55**, 12578 (1997); K. Yang and R. N. Bhatt, *Phys. Rev. Lett.* **80**, 4562 (1998).
- [12] S. R. White, *Phys. Rev. Lett.* **69**, 2863 (1992); *Phys. Rev. B* **48**, 10345 (1993); U. Schollwöck, *Rev. Mod. Phys.* **77**, 259 (2005).
- [13] see supplementary material available online.
- [14] F. J. Dyson, *Phys. Rev.* **92**, 1331 (1953).
- [15] J.-M. Luck, *Systèmes désordonnés unidimensionnels*, edited by Cea Saclay (Aléa-Saclay, Gif-sur-Yvette, 1992).
- [16] T. M. Nieuwenhuizen, *Physica* **113A**, 173 (1982); B. Derrida and E. Gardner, *J. Phys. (Paris)* **45**, 1283 (1984).
- [17] I. M. Lifshitz, *Soviet Physics Uspekhi* **7**, 549 (1965).
- [18] More precisely, it is important to stress that the binding of spinons, lifting the degeneracy between singlet and triplet states, is essentially due to the confinement interaction between spinons see eg Refs. 19. At the RMG point, this features is preserved since MG domains remain degenerate. Whatever the distance between the two spinons, the singlet and triplet states remain degenerate.
- [19] R. Chitra *et al.*, *Phys. Rev. B* **52**, 6581 (1995); D. Khomskii, W. Geertsma, M. Mostovoy, *Czech. J. Phys.* **46**, 3239 (1996); I. Affleck, in *Dynamical Dynamical Properties of Unconventional Magnetic Systems* (NATO ASI, Geilo, Norway, 1997). E. S. Sorensen, I. Affleck, D. Augier, and D. Poilblanc, *Phys. Rev. B* **58**, R14701 (1998); W. Zheng *et al.*, *Phys. Rev. B* **63**, 144411 (2001).
- [20] G. Uhrig, F. Schönfeld, M. Laukamp, and E. Dagotto, *Eur. Phys. J. B* **7**, 67 (1999).
- [21] A non-trivial exponent is expected and a specific statistical analysis should be carried out to provide correct results.
- [22] R. A. Hyman, K. Yang, R. N. Bhatt, and S. M. Girvin, *Phys. Rev. Lett.* **76**, 839 (1996); R. A. Hyman and K. Yang, *Phys. Rev. Lett.* **78**, 1783 (1997); M. Fabrizio and R. Mélin, *Phys. Rev. Lett.* **78**, 3382 (1997); C. Monthus, O. Golinelli, and T. Jolicœur, *Phys. Rev. Lett.* **79**, 3254 (1997); C. Monthus, O. Golinelli, and T. Jolicœur, *Phys. Rev. B* **58**, 805 (1998).
- [23] Y. Tang and A. W. Sandvik, *Phys. Rev. Lett.* **107**, 157201 (2011).

Supplementary material for: Localization of spinons in random Majumdar-Ghosh chains

Appendix A: Random variables features

For clarity, we list below the random variables that appear in the study, as well as their mean-value, variance and correlations with the β_i variable:

variable	mean	variance σ^2	correlations
β_i	β	σ_β^2 ($= \Delta^2/3$ for the box distribution)	
$\alpha_i = (1 - \lambda)(\beta_i + \beta_{i+1}) + \lambda\delta_i$	$\alpha = 2\beta$	$\sigma_\alpha^2 = 2\sigma_\beta^2$ (by choice)	$\overline{\alpha_i\beta_i} - \alpha\beta = (1 - \lambda)\sigma_\beta^2$
δ_i	$\delta = 2\beta$	$\sigma_\delta^2 = 2\frac{2-\lambda}{\lambda}\sigma_\beta^2$ (by choice of σ_α^2)	$\overline{\delta_i\beta_i} - \delta\beta = 0$
$\eta_i = \delta_i - \beta_i - \beta_{i+1}$	0	$\sigma_\eta^2 = \sigma_\delta^2 + 2\sigma_\beta^2 = \frac{4}{\lambda}\sigma_\beta^2$	$\overline{\eta_i\beta_i} = -\sigma_\beta^2$

Appendix B: Non-crossing dimer basis

1. $S_{\text{tot}} = 0$ sector and MG states

We gather some useful results on the non-crossing dimer basis used for variational calculations. Non-crossing dimer states form a non-orthogonal basis of the subspace with total spin $S_{\text{tot}} = 0$. In the MG physics, the states with dominant weights are rather simple as they are essentially states with nearest-neighbor dimers, with possibly slightly longer dimers locally. We also recall how the different terms of the Hamiltonian act on a MG state $|\text{MG}\rangle = |\cdots \bullet\bullet \bullet\bullet \bullet\bullet \bullet\bullet \bullet\bullet \cdots\rangle$ with dimers $|\bullet\bullet\rangle = \frac{1}{\sqrt{2}}[|\uparrow\downarrow\rangle - |\downarrow\uparrow\rangle]$. Applying a nearest neighbour term on a dimer, one simply recovers the MG state with eigenvalue $-3/4$. The same term applied between two dimers gives:

$$\mathbf{S}_i \cdot \mathbf{S}_{i+1} |\cdots \bullet\bullet \bullet\bullet \bullet\bullet \bullet\bullet \bullet\bullet \cdots\rangle = \frac{1}{4} |\cdots \bullet\bullet \bullet\bullet \bullet\bullet \bullet\bullet \bullet\bullet \cdots\rangle + \frac{1}{2} |\cdots \bullet\bullet \overbrace{\bullet\bullet} \bullet\bullet \bullet\bullet \cdots\rangle \quad (\text{B1})$$

Applying a next-nearest neighbour term, one gets :

$$\mathbf{S}_i \cdot \mathbf{S}_{i+2} |\cdots \bullet\bullet \bullet\bullet \bullet\bullet \bullet\bullet \bullet\bullet \cdots\rangle = \frac{1}{4} |\cdots \bullet\bullet \bullet\bullet \bullet\bullet \bullet\bullet \bullet\bullet \cdots\rangle - \frac{1}{2} |\cdots \bullet\bullet \overbrace{\bullet\bullet} \bullet\bullet \bullet\bullet \cdots\rangle, \quad (\text{B2})$$

which can be rewritten in the non-crossing dimer basis, using

$$|\cdots \bullet\bullet \overbrace{\bullet\bullet} \bullet\bullet \bullet\bullet \cdots\rangle = |\cdots \bullet\bullet \bullet\bullet \bullet\bullet \bullet\bullet \cdots\rangle + |\cdots \bullet\bullet \overbrace{\bullet\bullet} \bullet\bullet \bullet\bullet \cdots\rangle. \quad (\text{B3})$$

A useful overlap that will often appear in calculation is:

$$\langle \cdots \bullet\bullet \bullet\bullet \bullet\bullet \bullet\bullet \bullet\bullet \cdots | \cdots \bullet\bullet \overbrace{\bullet\bullet} \bullet\bullet \bullet\bullet \cdots \rangle = -1/2. \quad (\text{B4})$$

a. Deriving the Random Majumdar-Ghosh condition

Applying \mathcal{H} on the state $|\text{MG}\rangle$ which starts on even sites $2j$ gives

$$\mathcal{H}|\text{MG}\rangle = \frac{1}{4} \sum_j (-3\alpha_{2j} + \alpha_{2j+1} - \beta_{2j} - \beta_{2j+1}) |\text{MG}\rangle + \frac{1}{2} \sum_j (\alpha_{2j-1} - \beta_{2j} - \beta_{2j-1}) |[2j-2, 2j+1]\rangle,$$

where we write $|[2j-2, 2j+1]\rangle = |\cdots \bullet\bullet \overbrace{\bullet\bullet} \bullet\bullet \bullet\bullet \cdots\rangle$, the state with a dimer on bond $(2j-2, 2j+1)$. A similar expression is obtained for the other MG state. The RMG point is obtained by cancelling the second term.

b. *Some features of the Majumdar-Ghosh state*

We discuss some remarkable features of the MG state $|\text{MG}\rangle$ in the presence of disorder. From (B2) and (B4) and using and that $\sum_j(\dots) \rightarrow \frac{L}{2}\overline{(\dots)}$ for large enough system

$$\langle \text{MG} | \mathcal{H} | \text{MG} \rangle = E_{\text{MG}} = -\frac{3}{4} \sum_{j=1}^{L/2} \alpha_{2j-1} \rightarrow -\frac{3}{4} L \beta. \quad (\text{B5})$$

Notice that the above energy is exact even when (2) is not satisfied, but that the simplification from averaging only comes with the thermodynamic limit. In particular, it is remarkable that the energy remains independent of the disorder strength Δ . The fact that the MG state is not an eigenstate in general (when (2) is not satisfied) can be captured by calculating the energy dispersion of the state:

$$\sigma_{\text{MG}}^2 \equiv \langle \text{MG} | \mathcal{H}^2 | \text{MG} \rangle - E_{\text{MG}}^2 \rightarrow \frac{3L}{16} [\sigma_\alpha^2 + 2\sigma_\beta^2 + 2\alpha^2 + 8\beta^2 - 4(\overline{\alpha\beta} + \alpha\beta)] = \lambda \frac{3}{4} L \sigma_\beta^2 \quad (\text{B6})$$

Clearly, we do have $\sigma_{\text{MG}} = 0$ when (2) is fulfilled, as expected for an eigenstate.

2. $S_{\text{tot}} = 1/2$ sector and single spinon states

The single spinon dynamics is obtained using the restriction of the Hamiltonian on the subspace of states $|i\rangle = |\dots \bullet \bullet \bullet \uparrow \bullet \bullet \bullet \dots\rangle$ with spinon at position $2i+1$. We assume an infinite length chain, or a finite odd size chain with open boundary conditions, so that the spinon only moves on one sublattice. Periodic boundary conditions would only allow the spinon to change sublattice at the edges of the chain. Therefore it would just lead to a doubling of the effective size of the chain for the spinon. This method is variational as the family of states $|i\rangle$ does not form a complete family of subspace $\{S_{\text{tot}} = 1/2, S_{\text{tot}}^z = 1/2\}$. Moreover this family is free but is not orthogonal. The overlap between two states is

$$\langle i | j \rangle = \left(-\frac{1}{2} \right)^{|i-j|}. \quad (\text{B7})$$

Magnetization profiles $m_i = \frac{\langle \psi | S_i^z | \psi \rangle}{\langle \psi | \psi \rangle}$ can easily be computed [20] in this basis using :

$$\langle \psi | \psi \rangle = \sum_{j,k} \psi_k^* \psi_j \langle k | j \rangle, \quad (\text{B8})$$

$$\langle \psi | S_{2i+1}^z | \psi \rangle = \frac{1}{2} \sum_{k \leq i \leq j} \psi_k^* \psi_j \langle k | j \rangle + \text{c.c.}, \quad (\text{B9})$$

$$\langle \psi | S_{2i}^z | \psi \rangle = -\frac{1}{2} \sum_{k < i \leq j} \psi_k^* \psi_j \langle k | j \rangle + \text{c.c.}, \quad (\text{B10})$$

with $|\psi\rangle = \sum_i \psi_i |i\rangle$. If $|\psi_i|$ varies slowly compared to $(1/2)^i$, that is if the localization length is large ($\xi_{\text{spinon}} \gg 1/\ln 2$), the above sums can be approximated:

$$\langle \psi | \psi \rangle \simeq 3 \sum_i |\psi_i|^2, \quad (\text{B11})$$

$$\langle \psi | S_{2i+1}^z | \psi \rangle \simeq \frac{7}{2} |\psi_i|^2, \quad (\text{B12})$$

$$\langle \psi | S_{2i}^z | \psi \rangle \simeq -(|\psi_i|^2 + |\psi_{i-1}|^2). \quad (\text{B13})$$

In practice, these expressions work really well even for short localization lengths, and we did not need to compute the exact magnetization profiles. As the effective Hamiltonians are reals, all ψ_i are actually real numbers in our case.

Appendix C: Effective Hamiltonian for spinons

1. Projection on the variational subspace

We call P the orthogonal projector on the subspace generated by states $|i\rangle$. As an orthogonal projector, P is self-adjoint. The effective Hamiltonian for a single spinon $\tilde{\mathcal{H}}$ is the restriction of \mathcal{H} on this subspace :

$$\tilde{\mathcal{H}} = P\mathcal{H}P \quad (\text{C1})$$

We want to diagonalize $\tilde{\mathcal{H}}$ that is to find the energies E and the eigenstates $|\psi\rangle = \sum_i \psi_i |i\rangle$ so that

$$\tilde{\mathcal{H}}|\psi\rangle = E|\psi\rangle. \quad (\text{C2})$$

Of course, as \mathcal{H} is self-adjoint, $\tilde{\mathcal{H}}$ is also self-adjoint and the variational energies are real. If we write $|\psi\rangle$ as a variational wavefunction $|\psi\rangle = \sum_i \psi_i |i\rangle$, diagonalizing $[\tilde{\mathcal{H}}]_{ij}$ the matrix of $\tilde{\mathcal{H}}$ in the basis of states $|i\rangle$ is equivalent to solve the generalized eigenvalue problem :

$$\sum_i \langle j|\mathcal{H}|i\rangle \psi_i = E \sum_i \langle j|i\rangle \psi_i. \quad (\text{C3})$$

We insist on the fact that the matrices $\langle j|\mathcal{H}|i\rangle$ and $[\tilde{\mathcal{H}}]_{ij}$ are different because the basis of states $|i\rangle$ is not orthogonal. Indeed, it is useful in this context to introduce the matrix of overlaps \mathcal{O} which elements are $[\mathcal{O}]_{ij} = \langle i|j\rangle$. The search for eigenvalues in the generalized eigenvalue problem takes the form $\det(\mathcal{H} - E\mathcal{O}) = 0$ which is equivalent to $\det(\mathcal{O}^{-1}\mathcal{H} - E\mathbb{1}) = 0$. In addition, the projector on the subspace $\{|i\rangle\}$ is the inverse of the overlap matrix, ie. $P = \sum_{ij} [\mathcal{O}^{-1}]_{ij} |i\rangle\langle j|$. Then, $[\tilde{\mathcal{H}}]_{ij}$ is deduced from $\langle i|\mathcal{H}|j\rangle$ by

$$[\tilde{\mathcal{H}}]_{ij} = \sum_k [\mathcal{O}^{-1}]_{ik} \langle k|\mathcal{H}|j\rangle. \quad (\text{C4})$$

In the case of a chain, the inverse of \mathcal{O} has a simple tridiagonal form:

$$[\mathcal{O}^{-1}]_{ij} = \frac{1}{3} \begin{pmatrix} 4 & 2 & & & & \\ 2 & 5 & 2 & & & \\ & 2 & 5 & 2 & & \\ & & \ddots & \ddots & \ddots & \\ & & & 2 & 5 & 2 \\ & & & & 2 & 4 \end{pmatrix}, \quad (\text{C5})$$

which allows one to treat the problem analytically.

2. Effective Hamiltonian

We now detail how the terms of the Hamiltonian act on a single spinon state $|i\rangle$. Applying $\mathbf{S}_j \cdot \mathbf{S}_{j+1}$ on a spinon at position j , one gets

$$\mathbf{S}_j \cdot \mathbf{S}_{j+1} |\cdots \bullet \xrightarrow{\uparrow} \bullet \cdots\rangle = \frac{1}{4} |\cdots \bullet \xrightarrow{\uparrow} \bullet \cdots\rangle + \frac{1}{2} |\cdots \bullet \xrightarrow{\uparrow} \bullet \cdots\rangle \quad (\text{C6})$$

Using the following relation

$$|\cdots \bullet \xrightarrow{\uparrow} \bullet \cdots\rangle = |\cdots \bullet \xrightarrow{\uparrow} \bullet \cdots\rangle + |\cdots \bullet \xrightarrow{\uparrow} \bullet \cdots\rangle, \quad (\text{C7})$$

one can deduce the application of $\mathbf{S}_j \cdot \mathbf{S}_{j+2}$ in the variational basis :

$$\mathbf{S}_j \cdot \mathbf{S}_{j+2} |\cdots \bullet \xrightarrow{\uparrow} \bullet \cdots\rangle = -\frac{1}{4} |\cdots \bullet \xrightarrow{\uparrow} \bullet \cdots\rangle - \frac{1}{2} |\cdots \bullet \xrightarrow{\uparrow} \bullet \cdots\rangle \quad (\text{C8})$$

Applying $\mathbf{S}_{j-1} \cdot \mathbf{S}_{j+1}$ on a spinon at position j , one gets :

$$\mathbf{S}_{j-1} \cdot \mathbf{S}_{j+1} |\cdots \bullet \xrightarrow{\uparrow} \bullet \cdots\rangle = \frac{1}{4} |\cdots \bullet \xrightarrow{\uparrow} \bullet \cdots\rangle + \frac{1}{2} |\cdots \bullet \xrightarrow{\uparrow} \bullet \cdots\rangle \quad (\text{C9})$$

One can notice that this state is orthogonal to the variational subspace. As a result it simply disappears within the variational approach.

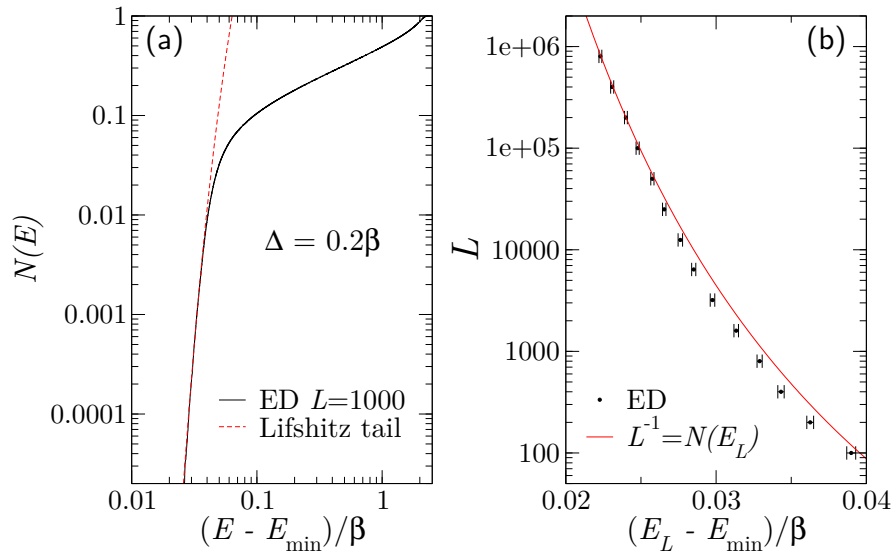


FIG. 4. (Color online) (a) Integrated density of states at low-energies compared with Lifshitz argument of Eq. (8). (b) Finite-size effects on the spinon energy.

d. A wrong argument for the susceptibility exponent at the random MG point

A naive argument for $\beta_{\min} < 0$ is the following : the susceptibility χ of the paramagnetic phase should correspond to independently filling spinons in single-spinon *Lifshitz states* up to zero energy. One is tempted to use a Lifshitz formula for $N(0)$, which is similar to (8) with the changes $E_\ell \simeq E_{\min} - \beta_{\min}\pi^2/2\ell^2$ and $E_{\min} = 9\beta_{\min}/4$. Using $\beta_{\min} = \Delta_c - \Delta$, with $\Delta_c = \beta$ the critical disorder strength, one gets for the susceptibility exponent $\phi = \pi\sqrt{2}/3 \simeq 1.481$ for the uniform distribution. Actually, such a prediction is wrong for the reason that the Lifshitz formula does not work close to the $E = 0$ while it does work close to E_{\min} . Indeed, when $\beta_{\min} \simeq 0$, the energy E_ℓ of a state in a cluster of size ℓ no longer depends on ℓ . This behavior is true whatever the smallness of the disorder strength. Instead, we observe that $N(E)$ is linear close to $E = 0$ and that $N(0)$ is rather linear with $\Delta - \Delta_c$. As discussed in the main text, the correct $N(0)$ is obtained by coupling the number of negative β s which leads to $\phi = 1$ for the uniform distribution.

4. Calculation of $\tilde{\mathcal{H}}_{\text{dim}}$

If we now want to do the same for the dimerization term of the Hamiltonian:

$$\mathcal{H}_{\text{dim}} = \sum_i \eta_i \mathbf{S}_i \cdot \mathbf{S}_{i+1}, \quad (\text{C13})$$

we have to consider states $|[2n-1, 2n+2], 2i+1\rangle$ ($n < i$) with a spinon at site $2i+1$ and a dimer on bond $(2n-1, 2n+2)$, and states $|2i+1, [2n, 2n+3]\rangle$ ($n > i$) with a spinon at site $2i+1$ and a dimer on bond $(2n, 2n+3)$. The overlaps of these states with states $|j\rangle$ are :

$$\langle j|[2n-1, 2n+2], 2i+1\rangle = -\frac{1}{2}\langle j|i\rangle(1 + 3\theta(n-j-1)) \quad (\text{C14})$$

$$\langle j|2i+1, [2n, 2n+3]\rangle = -\frac{1}{2}\langle j|i\rangle(1 + 3\theta(j-n-1)) \quad (\text{C15})$$

where θ is the Heaviside step function with the choice $\theta(0) = 1$. These states can be projected on the variational subspace.

$$P|[2n-1, 2n+2], 2i+1\rangle = -\frac{1}{2}|i\rangle - \left(-\frac{1}{2}\right)^{i-n+1}|n\rangle + \left(-\frac{1}{2}\right)^{i-n}|n-1\rangle \quad (\text{C16})$$

$$P|2i+1, [2n, 2n+3]\rangle = -\frac{1}{2}|i\rangle - \left(-\frac{1}{2}\right)^{n-i+1}|n\rangle + \left(-\frac{1}{2}\right)^{n-i}|n+1\rangle \quad (\text{C17})$$

Using these results, one can obtain the expression of $\tilde{\mathcal{H}}_{\text{dim}}$ in the variational basis :

$$\begin{aligned} \tilde{\mathcal{H}}_{\text{dim}}|i\rangle = & \left[-\frac{3}{4} \left(\sum_{n=0}^{i-1} \eta_{2n+1} + \sum_{n=i+1}^{\frac{L-1}{2}} \eta_{2n} \right) + \frac{1}{4} (\eta_{2i} + \eta_{2i+1}) \right] |i\rangle \\ & + \frac{1}{2} \eta_{2i} |i-1\rangle + \frac{1}{2} \eta_{2i+1} |i+1\rangle \\ & + \sum_{n=1}^{i-1} \left(-\frac{1}{2} \right)^{i-n} \eta_{2n} \left(\frac{1}{4} |n\rangle + \frac{1}{2} |n-1\rangle \right) \\ & + \sum_{n=i+1}^{\frac{L-3}{2}} \left(-\frac{1}{2} \right)^{n-i} \eta_{2n} \left(\frac{1}{4} |n\rangle + \frac{1}{2} |n+1\rangle \right) \end{aligned} \quad (\text{C18})$$

The energie due to the random dimerization η of a spinon localized at site $2i+1$ is :

$$\langle i | \mathcal{H}_{\text{dim}} | i \rangle = -\frac{3}{4} \left(\sum_{n=0}^{i-1} \eta_{2n+1} + \sum_{n=i+1}^{\frac{L-1}{2}} \eta_{2n} \right) \quad (\text{C19})$$

5. Numerical checks of one spinon in an open chain

As we have seen, the effet of \mathcal{H}_{dim} is to favor the creation of domains with spinons at the edges. If one considers an open chain with an odd number of sites, thus having one spinon, the effective model for the spinon is given by $\tilde{\mathcal{H}}_{\text{RMG}} + \lambda \tilde{\mathcal{H}}_{\text{dim}}$. The comparison of the variational approach with DMRG calculation is given on Fig. 5. The agreement is pretty good and we notice that because the confinement potential near its minimum behaves, to zero order approximation, almost linearly with the distance, one could expect that the tails of the wave-function are Airy function $\propto e^{-\frac{2}{3}((i-i_0)/\xi)^{3/2}}$ rather than pure exponential, with ξ a localization length. Fitting with a pure exponential gives a slightly worse fit (this would correspond to straight lines on this log plot).

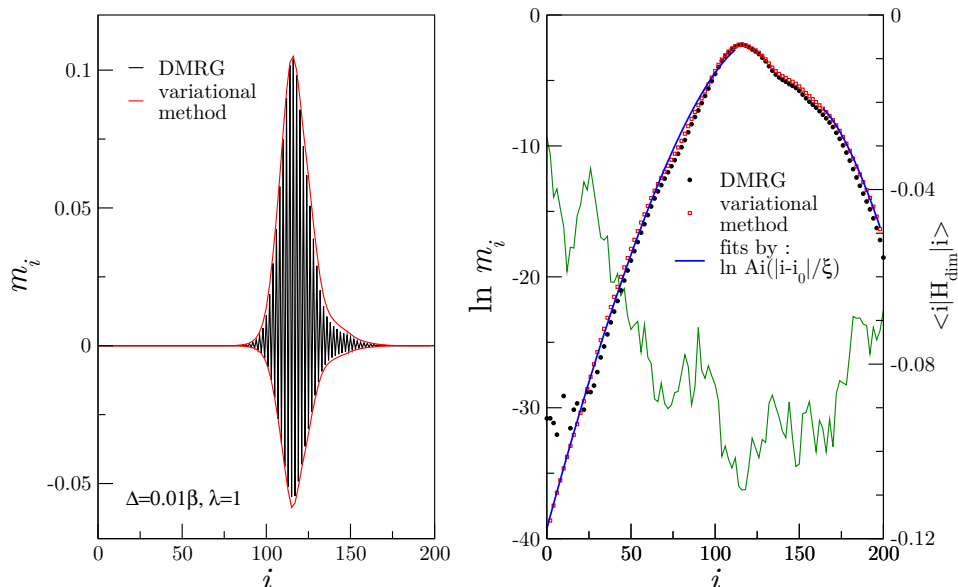


FIG. 5. (Color online) (a) Magnetization profile of a single spinon wave-function away from the RMG point. (b) Log plot showing fits by Airy functions and the effective local potential $\langle i | \mathcal{H}_{\text{dim}} | i \rangle$ coming from the dimerization Hamiltonian.

6. Energy of a long dimer state

We denote $|[2i-1, 2j]\rangle = |\dots \overbrace{\dots \dots \dots}^{2i-1} \dots \overbrace{\dots \dots \dots}^{2j} \dots\rangle$ the singlet product state with a long dimer between sites $2i-1$ and $2j$ ($i \leq j$). This state can be seen as a singlet state between two localized spinons. So, away from MG line ($\lambda > 0$), it may have a lower energy than the MG state. Let us apply the Hamiltonian on this state :

$$\begin{aligned}
\mathcal{H}|[2i-1, 2j]\rangle &= \frac{1}{4} \left(-3 \sum_{n=1}^{i-1} \alpha_{2n-1} + \sum_{n=1}^{i-2} (\alpha_{2n} - \beta_{2n} - \beta_{2n+1}) \right) |[2i-1, 2j]\rangle \\
&+ \frac{1}{2} \sum_{n=1}^{i-2} (\alpha_{2n} - \beta_{2n} - \beta_{2n+1}) |\dots \overbrace{\dots \dots \dots}^{2i-1} \dots \overbrace{\dots \dots \dots}^{2j} \dots\rangle \\
&+ \frac{1}{4} \left(-3 \sum_{n=i}^{j-1} \alpha_{2n} + \sum_{n=i+1}^{j-1} (\alpha_{2n-1} - \beta_{2n-1} - \beta_{2n}) \right) |[2i-1, 2j]\rangle \\
&+ \frac{1}{2} \sum_{n=i+1}^{j-1} (\alpha_{2n-1} - \beta_{2n-1} - \beta_{2n}) |\dots \overbrace{\dots \dots \dots}^{2i-1} \dots \overbrace{\dots \dots \dots}^{2j} \dots\rangle \\
&+ \frac{1}{4} \left(-3 \sum_{n=j+1}^{\frac{L}{2}} \alpha_{2n-1} + \sum_{n=j+1}^{\frac{L}{2}-1} (\alpha_{2n} - \beta_{2n} - \beta_{2n+1}) \right) |[2i-1, 2j]\rangle \\
&+ \frac{1}{2} \sum_{n=j+1}^{\frac{L}{2}-1} (\alpha_{2n} - \beta_{2n} - \beta_{2n+1}) |\dots \overbrace{\dots \dots \dots}^{2i-1} \dots \overbrace{\dots \dots \dots}^{2j} \dots\rangle \\
&+ \frac{1}{4} (\alpha_{2i-2} + \alpha_{2i-1} - \beta_{2i-2} - \beta_{2i} + \alpha_{2i-1} + \alpha_{2j} - \beta_{2i-1} - \beta_{2j+1}) |[2i-1, 2j]\rangle \\
&+ \frac{1}{2} [(\alpha_{2i-2} - \beta_{2i-2}) |[2i-3, 2j]\rangle + (\alpha_{2i-1} - \beta_{2i}) |[2i+1, 2j]\rangle] \\
&+ \frac{1}{2} [(\alpha_{2j-1} - \beta_{2j-1}) |[2i-1, 2j-2]\rangle + (\alpha_{2j} - \beta_{2j+1}) |[2i-1, 2j+2]\rangle] \\
&+ \frac{1}{4} (\beta_{2i-1} + \beta_{2j}) |[2i-1, 2j]\rangle \\
&+ \frac{1}{2} \left[\beta_{2i-1} |\dots \overbrace{\dots \dots \dots}^{2i-1} \dots \overbrace{\dots \dots \dots}^{2j} \dots\rangle + \beta_{2j} |\dots \overbrace{\dots \dots \dots}^{2i-1} \dots \overbrace{\dots \dots \dots}^{2j} \dots\rangle \right].
\end{aligned}$$

Of course, this state is not exactly an eigenstate but using

$$\langle [2i-1, 2j] | [2i-1 \pm 2, 2j] \rangle = \langle [2i-1, 2j] | [2i-1, 2j \pm 2] \rangle = -\frac{1}{2}, \quad (\text{C20})$$

one can calculate its energy :

$$\langle [2i-1, 2j] | \mathcal{H} | [2i-1, 2j] \rangle = -\frac{3}{4} \left(\sum_{n=1}^{i-1} \alpha_{2n-1} + \sum_{n=i}^{j-1} \alpha_{2n} + \sum_{n=j+1}^{L/2} \alpha_{2n-1} \right), \quad (\text{C21})$$

and compare it with the energy of the MG state :

$$\langle [2i-1, 2j] | \mathcal{H} | [2i-1, 2j] \rangle - \langle \text{MG} | \mathcal{H} | \text{MG} \rangle = \frac{3}{4} \left(\sum_{n=i}^j \alpha_{2n-1} - \sum_{n=i}^{j-1} \alpha_{2n} \right) \quad (\text{C22})$$

$$= \frac{3}{4} (\beta_{2i-1} + \beta_{2j}) + \frac{3}{4} \lambda \left(\eta_{2j-1} + \sum_{n=i}^{j-1} \eta_{2n-1} - \eta_{2n} \right). \quad (\text{C23})$$

Appendix D: On the convergence of DMRG calculations

DMRG calculations were performed using the finite-size algorithm, targeting one or two states (for instance to determine the singlet gap) and keeping typically from 400 to 1000 kept states. As MG are products of dimers, they have a simple matrix-product form which makes DMRG pretty efficient. The energies are converged to high precision. In the presence of localized spinons and in the $S^z = 0$ sector, the local magnetization should be zero everywhere. Yet, DMRG builds up a variational states with non-zero magnetization at the place of localized spinons. Indeed, due to the localization of spinons, triplet and singlet states are degenerate within an energy gap that is tiny (we observed gaps below $10^{-8}\beta$) and controlled by the residual magnetic couplings between spinons. Thus, the effective couplings between spinons become so tiny that it is extremely hard for DMRG to differentiate between the singlet or $S^z = 0$ triplet state and gives a superposition of these states as an output, with a finite local magnetization. Still, the spinon localization and magnetization profiles in the $S^z = 1$ are very well converged.

Appendix E: RSRG equations for the dimerized chain

Due to frustration, ferromagnetic couplings can be generated during the RSRG scheme so one has to take into account the possibility to generate spins higher than $1/2$. The renormalized couplings, which are here written in the general form J_{ij} , depend on the spin size s_i . We have the following two equations corresponding to the decimation scheme sketched in Fig. 6:

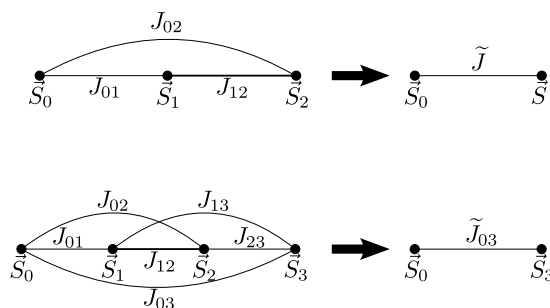


FIG. 6. Decimation scheme for the RSRG procedure of Model (1).

- if $s_1 \neq s_2$ or $J_{12} < 0$, we take $s = s_1 + s_2$ for $J_{12} < 0$ and $s = |s_1 - s_2|$ for $J_{12} > 0$ and we have

$$\tilde{J} = \frac{s(s+1) + s_1(s_1+1) - s_2(s_2+1)}{2s(s+1)} J_{01} + \frac{s(s+1) + s_2(s_2+1) - s_1(s_1+1)}{2s(s+1)} J_{02} \quad (\text{E1})$$

- if $s_1 = s_2$ and $J_{12} > 0$, we have

$$\tilde{J}_{03} = J_{03} + \frac{2}{3} s_1(s_1+1) \frac{(J_{01} - J_{02})(J_{23} - J_{13})}{J_{12}} \quad (\text{E2})$$

In particular for the first decimations, if α_i is the strongest coupling, spins i and $i+1$ are decimated and the renormalized couplings between remaining spins are :

$$\tilde{J}_{i-1,i+2} = \frac{(\alpha_{i-1} - \beta_i)(\alpha_{i+1} - \beta_{i+1})}{2\alpha_i} = \frac{(\beta_{i-1} + \lambda\eta_{i-1})(\beta_{i+2} + \lambda\eta_{i+1})}{2\alpha_i} \quad (\text{E3})$$

$$\tilde{J}_{i-2,i+2} = \frac{\beta_{i-1}(\alpha_{i+1} - \beta_{i+1})}{2\alpha_i} = \frac{\beta_{i-1}(\beta_{i+2} + \lambda\eta_{i+1})}{2\alpha_i} \quad (\text{E4})$$

$$\tilde{J}_{i-1,i+3} = \frac{(\alpha_{i-1} - \beta_i)\beta_{i+2}}{2\alpha_i} = \frac{(\beta_{i-1} + \lambda\eta_{i-1})\beta_{i+2}}{2\alpha_i} \quad (\text{E5})$$

$$\tilde{J}_{i-2,i+3} = \frac{\beta_{i-1}\beta_{i+2}}{2\alpha_i} \quad (\text{E6})$$

Thus for $\lambda = 0$, we end up with four degenerated couplings, implicitly reminiscent of the degeneracy of the MG domains at the RMG point, which makes the continuation of the RSRG procedure unstable numerically and ill-posed.

We have studied the behavior of the RSRG equations which lead to a large-spin Griffith phase but the details will be published elsewhere.

